

THE CONSTRUCTAL LAW AS AN APPROACH TO ADDRESS ENERGY EFFICIENCY IN THE URBAN FABRIC

Sylvie LORENTE

LMDC, INSA, 135 Avenue de Ranguueil, Toulouse 31077, France
E-mail: sylvie.lorente@insa-toulouse.fr

Abstract: Today 50% of the population lives in cities, while more than half of the energy consumption is spent on buildings. Even though these figures are well known, nothing changes. Needed is a paradigm shift able to address the multidisciplinary of the problem together with its multiscale aspects. Such paradigm lies within the Constructal law. In this work I will focus on applications of the Constructal law from the scale of the construction material to the scale of the urban district. I will demonstrate how the material can be designed in order to meet energy efficient requirements. Solutions for a better building envelope will be presented, together with the connection of different dwellings on the landscape in order to share the cooling/heating loads in an efficient fashion.

Key words: Multiscale design, Urban, Energy efficiency, Constructal.

1. INTRODUCTION

I view the city like a tapestry of multiscale flow systems with a finite amount of resources organized in a finite space. And flow systems are incredibly numerous in a city: flows of water, energy, power, flows of data and people. The city is an assembly of vascular systems distributed in a designed multiscale porous medium. Said in other words, in my view, the city is made of organisms superimposed and interconnected.

We learnt from thermodynamics that less useful energy is spent on the largest components of a system. Yet, in the same time, more useful energy is needed to carry this very component as its size increases. The sum of the two is minimum when they are of the same order of magnitude. From this tradeoff emerges the optimal size of the component. Exactly the same happens for the piece of material that composes the building, and for the building that is part of the city. The material itself may not be the most efficient one, just like the building itself may not be the most efficient. Yet, each of them must be considered within the built environment that surrounds them. When examined as an integral part of the city, the material or the building is an efficient organ working for the metabolism of the living tissue: the city.

For this reason, the design of a sustainable city calls for a shift in paradigm: working at one single scale is definitively not enough. The different scales must be considered together, in parallel. In this paper, I will illustrate this view through examples at material scale, building scale and district scale.

2. MATERIAL SCALE

Here I document the case of bio-based materials. This particular class of materials, and especially hemp concrete, is known for its expected moisture buffering capacity. Being able to model non isothermal moisture transport while accounting for the dominant parameters is therefore extremely important [1–3].

The model I wrote is based on the laws of mass conservation and energy conservation. Mass conservation is applied to the different phases that constitute the material: solid, air, liquid water and vapour water. Because usually the ability of the material to absorb humidity is measured as a function of the capillary pressure (from the relative humidity), the law of mass conservation for moisture is expressed as

$$\frac{\partial w}{\partial p_c} \frac{\partial p_c}{\partial t} = -\nabla \cdot \left[\left(\delta_l + \delta_v + \frac{\rho_v}{\rho_l} \right) \nabla p_c - \delta_v \left(\psi \frac{\partial p_{vsat}}{\partial T} - p_v \frac{\ln \psi}{T} \right) \nabla T - \frac{p_v}{p - p_v} \frac{M_v}{M_a} \delta_a p \right], \quad (1)$$

where w is the moisture content in (kg/m^3) of material, p_c is the capillary pressure (Pa), t is the time (s), δ_l and δ_v are the liquid and vapor water permeability respectively (s), ρ is the density (kg/m^3), ψ is the relative

humidity, T is the temperature, $\rho_v(T)$ is the vapor pressure, $\rho_{vsat}(T)$ is the vapor saturation pressure, M_v and M_a are respectively the molar mass (kg/mol) of vapor and air, δ_a is the air permeability of the material (s), and p is the total pressure (Pa).

The energy conservation reads

$$\left(\rho_s c_s + \sum_i w_i c_{p,i} \right) \frac{\partial T}{\partial t} = k_{mat} \nabla^2 T - \left[(c_{p,l} - c_{p,v}) T - L_v \right] S_l - \sum_i w_i \mathbf{V}_i c_{p,i} \nabla T, \quad (2)$$

where the subscript $i = 1$ for air, $i = 2$ for vapor and $i = 3$ for liquid, ρ_s is the solid density (kg/m³), c_s is the solid specific heat capacity (J/kg K), $c_{p,i}$ is the specific heat capacity at constant pressure of the different fluids (J/kg K), k_{mat} is the apparent thermal conductivity of the porous material, L_v is the latent heat of vaporisation (J/kg), and S_l is the water source (or sink) term (kg/(m³s)), and \mathbf{V} is the velocity vector (m/s). The source term S_l is obtained from the mass balance applied to liquid water only, combined to mass conservation for the solid ($\partial w / \partial t = 0$)

$$\left(\frac{1}{1 - \rho_v / \rho_l} \right) \frac{\partial w}{\partial t} = -\nabla \cdot (\delta_l \nabla p_c) \mp S_l. \quad (3)$$

The boundary conditions consist in the external (and internal) ambience conditions, namely temperature and relative humidity, heat transfer and mass transfer coefficients.

The objective is to design a porous construction material able to store moisture and release it later; this is the so-called moisture buffering capacity. In view of the Constructal law [4], the challenge consists in discovering the set of material characteristics that allows the highest moisture transfer performances. Those parameters are the material porosity, which will impact the capillary pressure, the absorption isotherm ($\partial w / \partial p_c$), the liquid permeability and the vapour permeability. Starting from the most classical construction material, concrete, we search for the material characteristics allowing to predict a moisture buffering capacity as high as possible. As an example, assume the material is wide enough to consider it as semi-infinite. The material is submitted to the following boundary conditions: Constant temperature $T = 22.6^\circ\text{C}$, relative humidity: 1 day at RH = 50% (initial conditions), followed by 9 days at RH = 75%, and 9 days at RH = 33%.

The system of equations together with the boundary and initial conditions are solved with a FEM package [5]. Plotted in Fig. 1 are the evolutions in time of the temperature and relative humidity at 50 mm from the surface. In addition to the imposed boundary conditions presented in the figures, we show the results obtained for the classical material (concrete), and for the designed material which transfer properties were improved. The temperature peak due to the phase change (water condensation) is noticed for the 2 materials although in a much weaker extend for concrete. The concrete is insensitive to the changes in relative humidity on its surface, unlike the designed material. It takes the latter 9 days to absorb almost entirely the increase in moisture due the sudden change in RH after day 1. Then the material slowly releases moisture in time, a behaviour accentuated within the depth of the material.

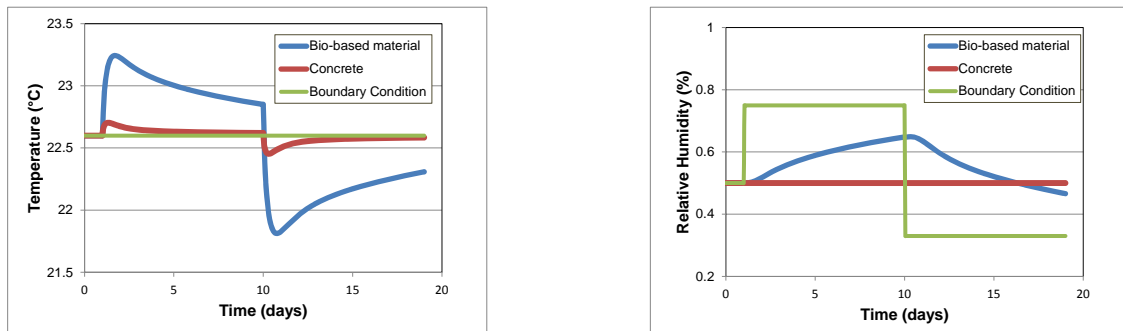


Fig. 1 – Temperature and relative humidity at 50 mm from the material surface.

3. BUILDING ENVELOPE SCALE

Ventilated cavities can be used for reducing the solar heat gains passing through the roof assembly. When an open ended air gap is placed below the tiles in a house or a building, then a current is formed due to buoyancy forces and part of the heat is removed by natural convection [6–8]. I view here an opportunity to introduce a

fundamental approach to the problem of naturally ventilated roof. By considering both the radiation and the convection heat exchanges, the theoretical analysis will help to determine the optimal air strip geometry.

The flow between two parallel vertical or quasi-vertical walls, with one wall receiving a constant heat flux q'' is driven by natural convection. This is also the case for a ventilated roof if we consider that the air slot is located between two walls inclined of an angle θ with the vertical. The two walls are made of panels of heights H , and width W . At first approximation we do not consider the walls thickness in the analysis that follows. The distance between the two walls is D (Fig. 2). We are looking for the optimal spacing D such that the ventilated air layer extracts as much heat as possible. The air outside the ventilated slot is at T_∞ . T_∞ is also the temperature at which air enters the bottom of the roof. The upper wall receives q'' . Heat is then transferred by natural convection along the wall and by radiation. Because $D \ll W$ and $D \ll H$, we consider that the radiation heat exchange is between the 2 walls of surface $W \times H$ separated by the distance D .

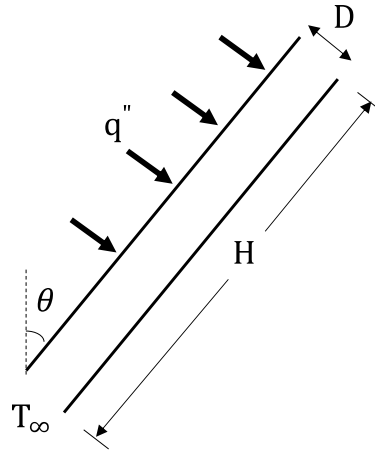


Fig. 2 – Inclined air layer.

We have

$$q''_{rad} = \frac{\sigma}{1/\varepsilon_H + 1/\varepsilon_c - 1} (\bar{T}_H^4 - \bar{T}_C^4), \quad (4)$$

where q''_{rad} is the radiation heat flux, σ is the Boltzmann constant, ε_H and ε_c are respectively the emissivity along the hot wall (upper plate of the channel) at the average temperature T_H , and the cold wall at T_H . According to [9] the ratio between the convection heat flux and the radiation heat flux in such a configuration is such that q''_{conv} represents 1/2 of q'' .

We invoke now scale analysis and write that, in an order of magnitude sense, the thermal boundary layer thickness along a wall of height H is

$$\delta_T \sim H Ra_{H^*}^{-1/5}, \quad (5)$$

$$Ra_{H^*} = \frac{g \cos \theta \beta q''_{conv} H^4}{\nu \alpha k}, \quad (6)$$

where Ra_{H^*} is the Rayleigh number β is the volumetric expansion coefficient, ν is the kinematic viscosity, α is the thermal diffusivity, k is the air thermal conductivity. When the spacing between the two walls is greater than $2\delta_T$, the air does not take advantage of the flow induced by natural convection, while a spacing between the two walls smaller than $2\delta_T$ would not use entirely the boundary layers development. In accord with the method of the intersection of asymptotes [10] we consider now 2 extreme cases. In the large spacing D limit, boundary layers develop independently along the 2 walls. Note that without radiation the temperature of the downer wall would be quasi identical to the inlet temperature T_∞ . The average Nusselt number along the hot wall is given by Vliet and Liu's correlation [11], and assuming that the convective heat transfer is quasi identical along the 2 walls, we obtain

$$q_{large D} \sim 1.5k Ra_{H^*}^{1/5} W (\bar{T}_H - T_\infty). \quad (7)$$

If the spacing between the walls is small enough, the boundary layers merge to create a chimney effect. Assume that T_{exit} is the air temperature at the exit of the slot. Because the external wall is heated, $T_{\text{exit}} > T_{\infty}$ and the air density at T_{exit} is lower than the air density at the channel inlet, $\rho(T_{\infty})$. We write that, $T_{\text{exit}} = T_{\infty} + \Delta T$, with ΔT the temperature increase along the air slot of height H . At the exit of the slot, the pressure difference is $\Delta P = \rho g \beta \Delta T H \cos \theta$. Considering the friction losses along the walls and combining them with energy conservation, we have

$$q_{\text{saml} D} \sim \left[\frac{\rho^2 g \beta \cos \theta}{f c_p} q_{\text{conv}}'' \right]^{1/3} D W c_p \Delta T. \quad (8)$$

The intersection of the 2 asymptotes represented by Eqs. (7) and (8) leads to the optimal spacing between walls D .

$$D_{\text{opt}} \sim \frac{(\bar{T}_H - T_{\infty})}{\Delta T} 1.5 \left(\frac{k}{c_p} \right) \text{HRa}_{H^*}^{-2/15} \left(\frac{f}{\rho^2 \nu \alpha} \right)^{1/3}. \quad (9)$$

4. DISTRICT SCALE

Ground Source Heat Pumps are part of the green buildings design strategies [12]. Typically, the building heat pump is coupled with an underground pipe network, which acts as a heat exchanger with the soil. At the scale of the district, connecting the building heat pumps to one single horizontal water loop is an interesting opportunity [13–16]. The heat exchanges through the loop can provide the base loads needs, while a conventional heating/cooling system in each connected building may supply the supplement peak demand.

Data centers house hundreds of computer servers, storage servers, etc. The corresponding heating gains are such that the internal load is higher than the heat losses through the buildings envelop, and the data centers need cooling all year round. Here we propose a methodology to design the underground loop network connecting a data center to several buildings in winter conditions [12]. Quantitatively, we assume that the buildings are classical office buildings without any specific energy efficient system. The heating needs are evaluated at 200 kWh/(m² year) with a total surface of 1 000 m² per building. This makes each office building heating need at about 23kW. The data center is assumed to have a small size with a heat pump rejecting 50 kW. The temperature of the fluid at the exit of each heat pump is known. Unknown is the flow system configuration such that the overall performance of the system is increased. The underground heat exchanger is a horizontal loop connecting the data center to the buildings. To illustrate the methodology we conduct the analysis in the case of two buildings, yet it can be expanded easily to more buildings. We developed the basis of the analytical part in [17]. As shown in Fig. 3, the data center heat pump connected to the loop rejects heat at a fluid temperature T_{Da} and with a mass flow rate mDa . The cold fluid comes from the two building heat pumps reject at respectively T_{B1} and T_{B2} with a mass flow rate \dot{m}_{B1} and \dot{m}_{B2} . On an axis attached to the loop, $x = 0$ is the location where the hot fluid from the data center is injected to the loop, noted A in Fig. 3. The first building is connected at a distance on the loop $x = L$, while the second building is connected at $x = 2L$. The way the 2 buildings are connected to the horizontal loop relatively to the data center is a degree of freedom: in Case 1, the first building heat pump extracts heat at a temperature T_{B1} , out at $x = L$, while the second building does the same at a temperature T_{B2} , out at the distance $x = 2L$ (Fig. 3a). In Case 2, the cold fluid is injected from the first building heat pump at T_{B1} and $x = L$. So does the second building heat pump at $x = 2L$ and $T = T_{\text{B2}}$ (Fig. 3b). In both cases $L_{\text{CD}} (= L_{\text{FA}})$ is a constant.

A baseline mass flow rate \dot{m}_0 circulates along the horizontal heat exchanger thanks to an auxiliary pump. According to the nomenclature in Fig. 3, we assume that the mass flow rate in the U-turn FA is \dot{m}_0 . The system of equations, based on the laws of mass and energy conservation, was solved in a non-dimensional form based on data listed in [12]. Note that we chose realistic values, which make the soil temperature between the exit temperatures of the datacenter and the buildings heat pumps.

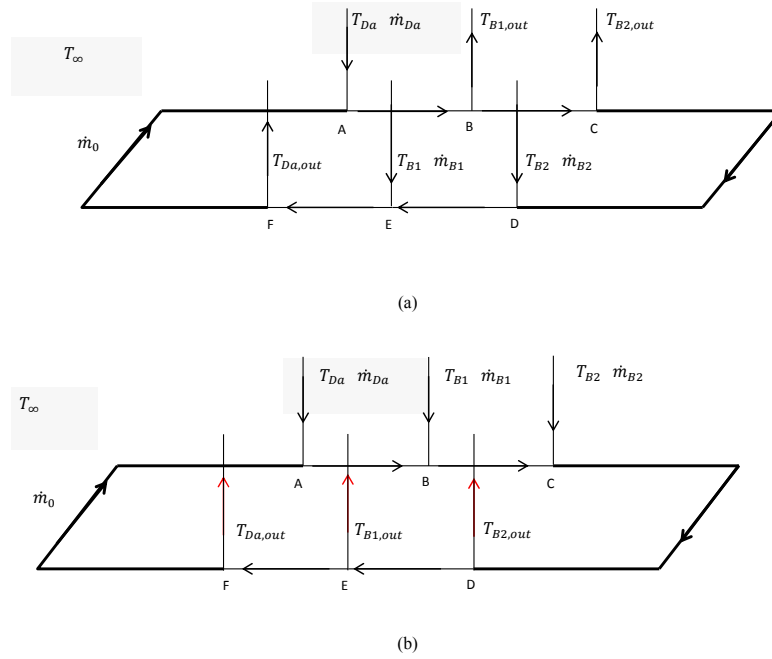


Fig. 3 – Two buildings heat pumps connected to a datacenter heat pump on the same loop [12].

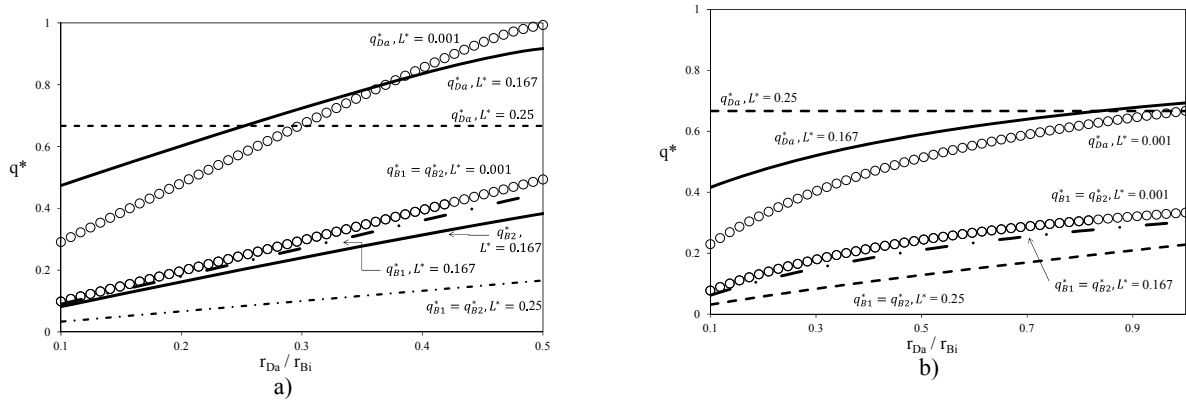


Fig. 4 – Non dimensional enthalpies q^* as a function of the mass flow rate ratio r_{Da}/r_{Bi} in: a) case 1; and b) case 2 [12].

Plotted in Fig. 4 are the non-dimensional enthalpies as a function of the ratio γ_{DA}/γ_{Bi} (here $\gamma_{B1} = \gamma_{B2}$) for different values of the length ratio $L^* = L/(4L + 2L_{FA})$. The two extreme cases correspond to $L^* \approx 0$ with buildings infinitely close to the datacenter, and $L^* \approx 0.25$ when $L \gg L_{FA}$. In the first case, the enthalpy provided by the datacenter is entirely given to the buildings, while the second extreme case corresponds to the maximum heat exchanges with the soil. The effect of the configuration on the results can be seen by comparing Fig. 4a to Fig. 4b, the latter corresponding to Case 2. The only difference between the two cases is the way the office buildings are connected to the loop. The network cannot provide the needed enthalpy exchanges in Case 2 whatever the loop length and whatever the mass flow rate ratio γ_{DA}/γ_{Bi} even though there is no ratio limitation in this case.

5. CONCLUSION

I believe that the solution to the design of sustainable living is to develop a holistic multi-scale and transdisciplinary approach to the city as a live flow system. Why multi-scale? We demonstrated in the past

that the sum of efficient elements – efficient in the sense of needing minimum power to operate – does not lead to the most efficient whole. The lesson taught by the examples developed in this paper is that each component must be envisaged hand-in-glove with its environment. From the constitutive material to the building envelope and the district/city scale, each object of study is like an organ working for the metabolism of the living body: the city.

ACKNOWLEDGEMENTS

I would like to thank the current and former students who contributed to this work: Billy Seng for the material scale section, Sylvia Slobodova for the envelope scale section, and Delphine Paludetto for the district scale section.

REFERENCES

1. JANSSEN H., BLOCKEN B., CARMELIET J., *Conservative modelling of the moisture and heat transfer in building components under atmospheric excitation*, International Journal of Heat and Mass Transfer, **50**, pp. 1128–1140, 2007.
2. OSANYINTOLA O.F., TALUKDAR P., SIMONSON C.J., *Effect of initial conditions, boundary conditions and thickness on the moisture buffering capacity of spruce plywood*, Energy and Buildings, **38**, pp. 1283–1292, 2006.
3. VAN BELLEGGHEM M., STEEMAN M., JANSSEN H., JANSSENS A., DE PAEPE M., *Validation of a coupled heat, vapour and liquid moisture transport model for porous materials implemented in CFD*, Building and Environment, **81**, pp. 340–353, 2014.
4. BEJAN A., LORENTE S., *Design with Constructal theory*, Wiley, 2008.
5. www.comsol.com
6. SUAREZ C., JOUBERT P., MOLINA J.L., SANCHEZ F.J., *Heat transfer and mass flow correlations for ventilated facades*, Energy and Buildings, **43**, pp. 3696–3703, 2011.
7. LEE S., PARK S.H., YEO M.S., KIM K.W., *An experimental study on airflow in the cavity of a ventilated roof*, Building and Environment, **44**, pp. 1431–1439, 2009.
8. BRANGEON B., JOUBERT P., BASTIDE A., *Influence of the dynamic boundary conditions on natural convection in an asymmetrically heated channel*, International Journal of Thermal Sciences, **95**, pp. 64–72, 2015.
9. KRISHNAN, PREMACHANDRAN B., BALAJI C., VENKATESHAN S.P., *Combined experimental and numerical approaches to multi-mode heat transfer between vertical parallel plates*, Experimental Thermal and Fluid Sciences, **29**, pp. 75–86, 2004.
10. BEJAN A., *Convection Heat Transfer*, 4th Ed., Wiley, 2013.
11. VLIET G.C., LIU C.K., *An experimental study of turbulent natural convection boundary layers*, Journal of Heat Transfer, **91**, pp. 517–531, 1969.
12. PALUDETTO D., LORENTE S., *Modeling the heat exchanges between a datacenter and neighboring buildings through an underground loop*, Renewable Energy, **93**, pp. 502–509, 2016.
13. G. FLORIDES, S. KALOGIROU, *Ground heat exchangers – a review of systems, models and applications*, Renewable Energy, **32**, pp. 2461–2478, 2007.
14. HUA Q., YUNGANG W., *Modeling the interactions between the performance of ground source heat pumps and soil temperature variations*, Energy for Sustainable Development, **23**, pp. 115–131, 2014.
15. SONI S.K., PANDEY M., BARTARIA V.N., *Ground coupled heat exchangers: a review and applications*, Renewable Sustainable Reviews, **47**, pp. 83–92, 2015.
16. ALAVY M., DWORKIN S.B., LEONG W.H., *A design methodology and analysis of combining multiple buildings onto a single district hybrid ground source heat pump system*, Renewable Energy, **66**, pp. 515–522, 2014.
17. ALMERBATI A., LORENTE S., ANDERSON R., BEJAN A., *Energy design for dense neighborhoods: one heat pump rejects heat, the other absorbs heat from the same loop*, International Journal of Thermal Sciences, **96**, pp. 227–235, 2015.